

## Derivation of aerosol optical properties from multi-wavelength lidar observations

H. Kinjo\*, M. Yabuki, H. Kuze, and N. Takeuchi\*

Center for Environmental Remote Sensing, Chiba University

1-33 Yayoi-cho, Inage-ku, 263-8522 Japan

\*E-mail: [wood@ceres.cr.chiba-u.ac.jp](mailto:wood@ceres.cr.chiba-u.ac.jp)

### ABSTRACT

A multi-wavelength Mie lidar is a powerful tool to investigate the optical properties of aerosol particles along with their vertical profile information. In the usual analysis with the Fernald method, however, it is required to assume both the extinction-to-backscattering ratio (lidar ratio,  $S_1$ ) and the extinction coefficients at the far end boundary. For a multi-wavelength lidar, appropriate choices of these parameters are indispensable to derive consistent profiles from the actual data. In this work, we propose two algorithms for the analysis of four-wavelength lidar data. The first approach is a pragmatic one, and it relies on the sun photometer data simultaneously measured with the lidar data. By assuming a constant  $S_1$  value for each wavelength in the lower troposphere, a consistent set of  $S_1$  is determined by fitting the observed profiles to reference profiles that are relevant to the aerosol optical thicknesses from the sun photometer measurement. The second algorithm is more comprehensive in that it adopts the direct fitting of the lidar A-scopes to the theoretical curves that are based on a look-up table: the table is pre-calculated for various combinations of the extinction coefficient,  $S_1$  parameter, complex refractive index, and aerosol size distribution. As a result, the vertical profiles of these parameters are determined along with the extinction profile.

### 1. INTRODUCTION

Mie-scattering lidars provide extinction profiles of atmospheric aerosols. For the inversion of the lidar data to give the aerosol extinction, Fernald<sup>1)</sup> methods are commonly employed. In this method, it is necessary to postulate a lidar ratio, also known as the  $S_1$  parameter. For particle size distributions and refractive indices of tropospheric aerosols, Mie calculations show that the values of the  $S_1$  parameter can vary in a range of 10 to 100 sr. This wide range implies uncertainty of more than a factor of 10 in the retrieved optical thickness, obviously too large to provide reliable information on aerosol extinction profiles for many practical purposes. Knowledge of the lidar ratio is essential for the interpretation of the lidar data. Since it is by no means possible to determine the lidar ratio only from the elastic backscattering lidar measurements, practical calibration methods have to be contrived. In regard to this, two complementary, alternative approaches are available. First, the optical thickness data from a sun photometer can be used to calibrate the lidar data. Second, the Mie theory can be employed to calculate the aerosol optical properties beforehand.

In the first approach, a sun photometer is used to observe the aerosol optical thickness simultaneously with the lidar observation. Then, the  $S_1$  parameter is specified by matching the optical thickness  $\tau$  derived from the lidar measurement with that from the sun photometer<sup>2)</sup> (hereafter we call this the “ $\tau$ -matching method”).

In the second approach, the aerosol optical properties (extinction coefficient, scattering coefficient,  $S_1$  parameter, and so on) are calculated by the Mie theory<sup>3)</sup>, assuming a certain aerosol size distribution (ASD) and complex refractive index. So far, a number of attempts have been made to combine lidar measurements and Mie calculations. Sasano and Bowell<sup>4)</sup> showed the capability of a multi-wavelength lidar for discriminating between several aerosol types using the wavelength dependence of aerosol backscatter coefficients. Qing *et al.*<sup>5)</sup> simulated numerically the derivation of the ASD from multi-wavelength lidar data, and discussed the errors in the derived size distribution. Rajeev and Parameswaran<sup>6)</sup> retrieved the altitude profile of aerosol extinction and the shape of ASD using two iterative methods.

The atmospheric data collection lidar (ADCL)<sup>7,8)</sup> at the Center for Environmental Remote Sensing, Chiba University, provides information on tropospheric aerosols at wavelengths of 355, 532, 756 and 1064 nm. The system is designed to monitor the aerosol in the lower troposphere, the contribution from which is essential for the atmospheric correction of satellite remote sensing data. In the present work, we propose two methods for the analysis of multi-wavelength lidar data employing the ADCL case for our simulation and demonstration. Nevertheless, it is emphasized that our approach could in principle be applied to any other multi-wavelength lidar systems.

The first algorithm<sup>9)</sup> utilizes the sun photometer data simultaneously measured with the lidar data. Since a sun photometer provides multi-wavelength optical thickness data, its use as a calibration tool in the multi-wavelength lidar

measurements might seem straightforward at first glance. Practically speaking, however, this is not always the case. Even when a sufficient range is covered for a wavelength near the center of the visible spectrum (e.g. at 532 nm), the situation becomes worse for longer wavelengths because of the degradation of the detector sensitivity. For shorter wavelength, on the other hand, larger extinction due to the molecular scattering and absorption tend to hinder sufficient range coverage. For these wavelengths it may happen that the range of lidar data is too limited to infer the optical thickness which is to be compared with the sun photometer data. To alleviate such difficulties associated with the wavelength, here we propose a "reference profile" method, which is based on the simultaneous measurement using a multi-wavelength lidar and a sun photometer. In the analysis, we postulate that for each wavelength, the value of the  $S_1$  parameter is constant in the entire troposphere. The parameter at 532 nm is determined by comparing the data from the two instruments (the  $\tau$ -matching method, as mentioned above). To obtain the reference profile, we assume that at each altitude, the aerosol extinction coefficients for the other wavelengths (355, 756, and 1064 nm) are proportional to the coefficient at 532 nm. The proportional factors are given by the ratio between the optical thickness at each wavelength and that at 532 nm. On the other hand, the lidar signals for the three wavelengths are separately analyzed with the Fernald method by changing  $S_1$  in a plausible range. By minimizing the difference between this retrieved profile and the reference profile, it becomes possible to determine the  $S_1$  parameter.

The second algorithm<sup>10)</sup> utilizes a look-up table (LUT) to derive vertical distributions of aerosol optical parameters in the troposphere. The LUT is calculated by the Mie theory for 11 types of aerosol size distributions and 3000 values of the imaginary part of the complex refractive index. The analysis of multi-wavelength lidar signals is accomplished by directly fitting the lidar A-scopes to the theoretical curves that are based on the look-up table. At each altitude, not only the aerosol extinction coefficient but also the  $S_1$  parameter, the imaginary part of the complex refractive index, and the ASD are derived from this procedure. These include most of the important information on the aerosol optical properties. In this respect, this algorithm exhibits quite a unique feature among the analysis methods of multi-wavelength lidar data. The resulting optical parameters, however, are dependent on the parameters that are used to pre-calculate the LUT. This infers that in order to attain reasonable results, it is indispensable to prepare a LUT which is representative of the actual aerosol properties. For this purpose conventional approaches such as the reference profile method are useful for the first-step analysis of multi-wavelength lidar data.

## 2. THEORY

### 2.1. Fernald Analysis

Here we briefly summarize the analysis of lidar signals utilizing the Fernald method.<sup>1)</sup> This algorithm is mainly required for the implementation of the reference profile method (Sec. 2.2). The single scattering lidar equation is given by

$$P(z) = K \frac{G(z)}{z^2} [\beta_1(z) + \beta_2(z)] \times \exp \left[ -2 \int_{z_0}^{z_r} \alpha_1(z') dz' - 2 \int_{z_0}^{z_r} \alpha_2(z') dz' \right], \quad (1)$$

where  $K$  is a system constant,  $G(z)$  the geometric form factor,  $z$  the range from the lidar to the target, and  $\beta_j$  and  $\alpha_j$  ( $j=1,2$ ) are the backscattering and extinction coefficients, respectively: subscripts 1 and 2 refer to the aerosol particles and molecules, respectively. We assume a linear relation between  $\beta_j$  and  $\alpha_j$ :

$$\alpha_j = S_j \beta_j, \quad (2)$$

where  $S_j$  is the extinction-to-backscattering ratio. The molecular coefficients ( $\beta_2$  and  $\alpha_2$ ) can be obtained from standard atmospheric data. We define the range-corrected signal as  $X(z) \equiv P(z)z^2$ . The aerosol extinction coefficient can be derived as

$$\alpha_1(z) = -\frac{S_1(z)}{S_2} \alpha_2(z) + \frac{S_1(z)X(z) \exp [I(z)]}{\frac{X(z_r)}{\frac{\alpha_1(z_r)}{S_1(z_r)} + \frac{\alpha_2(z_r)}{S_2}} + J(z)}, \quad (3)$$

where the integrals  $I(z)$  and  $J(z)$  are defined as

$$I(z) = 2 \int_z^{z_r} \left[ \frac{S_1(z')}{S_2} - 1 \right] \alpha_2(z') dz', \quad (4)$$

and

$$J(z) = 2 \int_z^{z_f} S_1(z') X(z') \exp[-I(z')] dz' \quad (5)$$

In these equations,  $z_f$  refers to the far-end boundary altitude at which a value is assumed for the aerosol extinction  $\alpha_1(z_f)$ .

## 2.2. Reference profile method

The  $S_1$  parameter at 532 nm is determined by adjusting it in the Fernald analysis of the lidar data at 532 nm so that the resultant optical thickness agrees with that from the simultaneously measured sun photometer data. The aerosol extinction profile  $\alpha_1^{(\text{Obs})}(\lambda_{532}, z)$  can also be determined in this manner.

The reference profile for each wavelength  $\alpha_1^{(\text{Obs})}(\lambda_{532}, z)$  ( $j = 355, 756, \text{ and } 1064$ ) is defined as follows:

$$\alpha_1^{(\text{Ref})}(\lambda_j, z) = C_j \alpha_1^{(\text{Obs})}(\lambda_{532}, z), \quad (6)$$

where  $C_j = \tau(\lambda_j)/\tau(\lambda_{532})$  with  $\tau(\lambda_{532})$  and  $\tau(\lambda_j)$  representing the optical thickness at  $\lambda_{532}$  and at  $\lambda_j$  as derived from the sun photometer data. On the other hand, the Fernald analysis of the data at  $\lambda_j$  yields an ‘‘observed’’ profile of  $\alpha_1^{(\text{Obs})}(S_1, \lambda_j, z)$ . When  $\alpha_1^{(\text{Obs})}(S_1, \lambda_j, z)$  is retrieved from the lidar signal, we employ the value of  $\alpha_1^{(\text{Ref})}(\lambda_j, z)$  at the far-end boundary. Then the difference between  $\alpha_1^{(\text{Obs})}(S_1, \lambda_j, z)$  and  $\alpha_1^{(\text{Ref})}(\lambda_j, z)$  is considered using a function

$$D_j(S_1) = \left\{ \frac{1}{N} \sum_{l=m}^n [\alpha_1^{(\text{Obs})}(S_1, \lambda_j, z_l) - \alpha_1^{(\text{Ref})}(\lambda_j, z_l)]^2 \right\}^{1/2} \times \left[ \frac{1}{N} \sum_{l=m}^n \alpha_1^{(\text{Ref})}(\lambda_j, z_l) \right]^{-1}, \quad (7)$$

where  $m$  and  $n$  denote the initial (the lowest altitude) and the final (the highest altitude) data number of the fitting, respectively, with  $N$  indicating  $n - m + 1$ . For each wavelength, the value of  $S_1$  is determined by the condition that one obtains a minimum value of  $D_j(S_1)$  in a plausible range of  $S_1$ .

## 2.3. LUT method

### 2.3.1. Construction of LUT

A look up table (LUT) is constructed by means of the Mie-scattering theory. Table 1 summarizes the parameters used to calculate the present LUT. For the ASD  $n(r)$ , we take the urban and maritime model<sup>11)</sup> as two extreme cases, and nine intermediate cases are defined by logarithmically interpolating between the two. The real part of the aerosol refractive index ( $m'$ ) is fixed at 1.50, representing an average value usually obtained from the ground sampling. The imaginary part ( $m''$ ), on the other hand, is allowed to vary between 0.0 and 0.03, with a step of  $1.0 \times 10^{-5}$ . This small step size is necessary to deal with the rapid changes in the wavelength dependence of the optical parameters derived from the LUT analysis. For simplicity, we neglect the wavelength dependence of the refractive index.

Using the Mie-scattering theory<sup>3)</sup>, we calculate the extinction coefficient  $\alpha_1$  and the  $S_1$  parameter for each  $n(r)$ ,  $m''$ , and wavelengths  $\lambda$  (355, 532, 756, 1064 nm). A table consists of a set of  $\alpha_1$  and  $S_1$  parameters for the four wavelengths calculated with the same size distribution and the refractive index. The values of  $\alpha_1$  are normalized to the value for 532 nm. In the following, we denote the (normalized) extinction coefficient and  $S_1$  parameter of the table data as  $e_i(\lambda(i), m(j), s(u))$  and  $S_1(\lambda(i), m(j), s(u))$ , respectively. Here  $\lambda(i)$  indicates the wavelength ( $i=1$  for 355,  $i=2$  for 532 nm,  $i=3$  for 756 nm, and  $i=4$  for 1064 nm),  $m(j)$  the refractive index ( $j=0, 1, \dots, 3000$ ),  $s(u)$  the size distribution model ( $u=0$  for the urban, ...  $u=10$  for the maritime).

**Table 1.** Parameters used to calculate LUT.

<b>* Size distribution</b>				
	<i>i</i>	$N_0$	$r_g$	$\sigma$
Urban aerosol model <sup>11)</sup>	1	$9.93 \times 10^4$	0.00651	0.245
	2	$1.11 \times 10^3$	0.00714	0.666
	3	$3.64 \times 10^4$	0.0248	0.337
Maritime aerosol model <sup>11)</sup>	1	$1.33 \times 10^2$	0.0039	0.657
	2	$6.66 \times 10^1$	0.0133	0.210
	3	$3.06 \times 10^0$	0.29	0.396

$$\frac{dN}{d \log r} = \sum_{i=1}^3 \frac{N_{0i}}{\sqrt{2\pi}\sigma_i} \exp \left[ -\frac{(\log r / r_{g,i})^2}{2\sigma_i^2} \right]$$

Division of each model into 10 logarithmically ( $u=0$  to  $10$ ).

$s(0)$  : Urban model , ... ,  $s(u)$ , ... ,  $s(10)$  : Maritime model

**\* Complex refractive index**

Real part: 1.50

Imaginary part: 0.00000 to 0.03000 (step 0.00001)

**\* Wavelength**

355, 532, 756 and 1064nm

### 2.3.2. LUT method

The altitude  $z$  is considered in a discrete way of  $z(q)$  ( $q = 1, 2, \dots, Q$ ) with  $z_1 = z(1)$  being the lowest altitude in the analysis. In order to avoid the effect of the lidar overlapping function, we assume that  $z_1$  is taken at an altitude where  $G(z)$  becomes unity. Moreover, we assume that for every wavelength,  $\alpha_1(z_1) = \alpha_1(z_2)$  and  $S_1(z_1) = S_1(z_2)$ : for all the altitudes below  $z_2$ ,  $\alpha_1$  and  $S_1$  are postulated to be constant. Under these assumptions, the aerosol optical parameters are determined as described below. In the following, the extinction coefficient,  $S_1$  parameter, refractive index, size distribution, and the signal power are written as  $\alpha_1^*(z(q), \lambda(i))$ ,  $S_1^*(z(q), \lambda(i))$ ,  $n^*(z(q), \lambda(i))$ ,  $P_{cal}^*(z(q), \lambda(j))$ , respectively.

#### 2.3.2.1. Determination of the initial parameters

First we determine the initial values of  $\alpha_1^*(z_1, \lambda(i)) = \alpha_1^*(z_2, \lambda(i))$  and  $S_1^*(z_1, \lambda(i)) = S_1^*(z_2, \lambda(i))$ . Since the extinction coefficient in the LUT is normalized to the value of 532 nm, we apply a factor  $C(t)$  to convert the value to the actual extinction coefficient. Here,  $C(t)$  is varied between  $5.0 \times 10^{-6}$  to  $1.0 \times 10^{-3}$  (in units of  $m^{-1}$ ) with a step of  $5.0 \times 10^{-6}$  (i.e.  $t = 0 \sim 200$ ). Thus, the aerosol extinction is given by  $C(t) \cdot e_1(\lambda(i), m(j), s(u))$ . Combining this extinction coefficient with the  $S_1$  parameter,  $S_1(\lambda(i), m(j), s(u))$ , the signal intensity at the altitudes  $z_1$  and  $z_2$  are calculated as

$$P_{cal}(z(q), \lambda(i), m(j), s(u), C(t)) = \frac{K}{z(q)^2} \left[ \frac{C(t) \cdot e_1(\lambda(i), m(j), s(u))}{S_1(\lambda(i), m(j), s(u))} + \frac{\alpha_2(z(q), \lambda(j))}{S_2} \right] \times \exp \left[ -2 \int_0^{z(q)} C(t) \cdot e_1(\lambda(i), m(j), s(u)) dz' - 2 \int_0^{z(q)} \alpha_2(z') dz' \right]_{q=1,2} \quad (8)$$

We define an error,  $Err$ , as the summation over the four wavelengths of the difference between the calculated ratio of the signal intensity and the observed ratio of the signal intensity.

$$Err = \sum_{j=1}^4 \left[ \frac{P_{cal}(z(2), \lambda(i), m(j), s(u), C(t))}{P_{cal}(z(1), \lambda(i), m(j), s(u), C(t))} - \frac{P_{obs}(z(2), \lambda(i))}{P_{obs}(z(1), \lambda(i))} \right]^2 \quad (9)$$

Note that the system constant  $K$  in eq. (1) is eliminated owing to the form of eq. (9). The value of  $Err$  is calculated for all the possible combinations of  $j = 0 \sim 3000$ ,  $u = 0 \sim 10$ , and  $t = 0 \sim 200$ . We determine the parameters at  $z_1$  and  $z_2$  from the

condition that  $Err$  takes a minimum value ( $j=J$ ,  $u=U$ , and  $t=T$ ). Therefore, we have

$$\left\{ \begin{array}{l} \alpha_1^*(z(1,2), \lambda(i)) = C(T) \cdot e_1(\lambda(i), m(J), s(U)) \\ S_1^*(z(1,2), \lambda(i)) = S_1(\lambda(i), m(J), s(U)) \\ m^*(z(1,2)) = m(J) \\ s^*(z(1,2)) = s(U) \\ P_{cal.}^*(z(1,2), \lambda(j)) \\ \quad = P_{cal.}(z(1,2), \lambda(i), m(J), s(U), C(T)) \end{array} \right. \quad (10)$$

### 2.3.2.2. Successive determination of the parameters

Second, we apply the method in a successive way to determine the aerosol parameters at altitudes  $z(q)$  ( $q \geq 3$ ). The signal power at  $z(q)$  is calculated as

$$P_{cal.}(z(q), \lambda(i), m(j), s(u), C(t)) = \frac{K}{z(q)^2} \left[ \frac{C(t) \cdot e_1(\lambda(i), m(j), s(u))}{S_1(\lambda(i), m(j), s(u))} + \frac{\alpha_2(z(q), \lambda(j))}{S_2} \right] \quad (11)$$

$$\times \exp \left[ -2 \left( \int_0^{z(q-1)} \alpha_1^*(z', \lambda(j)) dz' + \int_0^{z(q-1)} \alpha_2(z') dz' \right) - 2 \left( \int_{z(q-1)}^{z(q)} C(t) \cdot e_1(\lambda(i), m(j), s(u)) dz' + \int_{z(q-1)}^{z(q)} \alpha_2(z') dz' \right) \right]_{q \geq 3}$$

Since the extinction  $\alpha_1^*$  is already known below the altitude of  $z(q-1)$ , it is only required to determine the parameters at  $z(q)$ . In this case, we introduce an error function defined as

$$Err. = \sum_{q'=1}^{q-1} \sum_{i=1}^4 \left[ \frac{P_{cal.}(z(q), \lambda(i), m(j), s(u), C(t))}{P_{cal.}^*(z(q'), \lambda(i))} - \frac{P_{obs.}(z(q), \lambda(i))}{P_{obs.}(z(q'), \lambda(i))} \right]^2 \quad (12)$$

Namely, the squared difference between the ratio of the calculated signal intensities and the ratio of the observed signal intensities is summed over the altitudes below  $z(q-1)$  and over the wavelengths. The reason we employ the altitude below  $z(q-2)$  is to hold down the noise effects. The minimum of  $Err$  is sought by changing the indices  $j$ ,  $u$ , and  $t$ , as in the case of eq. (8) (the values of indices are determined to be  $J$ ,  $U$ , and  $T$ , respectively). In this manner, the aerosol parameters at the altitude  $z(q)$  are obtained to be

$$\left\{ \begin{array}{l} \alpha_1^*(z(q), \lambda(i)) = C(T) \cdot e_1(\lambda(i), m(J), s(U)) \\ S_1^*(z(q), \lambda(i)) = S_1(\lambda(i), m(J), s(U)) \\ m^*(z(q)) = m(J) \\ s^*(z(q)) = s(U) \\ P_{cal.}^*(z(q), \lambda(j)) \\ \quad = P_{cal.}(z(q), \lambda(i), m(J), s(U), C(T)) \end{array} \right. \quad (13)$$

By use of the parameters in eqs. (10) and (13) and the size distribution function  $ns(r)$  for the model distribution  $s^*(z(q))$ , the size distribution at an altitude  $z(q)$  can be derived as

$$n^*(r, z(q)) = ns(r) \frac{\alpha_1^*(z(q), \lambda(j))}{\int_0^{\infty} ns(r) \cdot \sigma_{ext}(r, \lambda(j)) dr} \quad (14)$$

Thus, all the aerosol parameters have been determined at  $z(q)$ . A similar procedure is applied at a next altitude of  $z(q+1)$ . The parameters are obtained in this manner at each altitude up to  $z(Q)$ .

### 3. RESULTS AND DISCUSSION

#### 3.1. Reference method

##### 3.1.1. Simulation of the reference profile method

In this section, we describe the result of a simulation in which the influence of atmospheric as well as operational parameters is examined for the reference profile method. As for the vertical distribution of aerosol extinction, we use model profile at 355 and 532 nm. The model extinction coefficient is assumed to be constant in the mixed boundary layer (MBL) up to 1500 m. In the free troposphere, the extinction coefficient is postulated to decrease exponentially with the altitude. For 532 nm, the extinction value in this layer is changed in five ways:  $\alpha_1^{(\text{Model})}(\lambda_{532}, \text{MBL}) = 1.0 \times 10^{-4}$ ,  $2.5 \times 10^{-4}$ ,  $5.0 \times 10^{-4}$ ,  $7.5 \times 10^{-4}$ , and  $1.0 \times 10^{-3} \text{ m}^{-1}$ . (Hereafter these are named as models 1-5.)

By using these model profiles (and the wavelength dependence of  $\alpha_1$  and  $S_1$  parameters, as explained below), lidar signals are simulated and analyzed with the Fernald method to obtain  $\alpha_1^{(\text{Obs})}(\lambda_j, z)$ . At the same time, the total optical thickness is derived for each wavelength, yielding the proportional constant  $C_j$  in eq. (6).

The wavelength dependence of the extinction and the value of  $S_1$  parameter are calculated by means of the Mie scattering theory. In MBL, an aerosol refractive index of  $1.5 - 0.05i$  is assumed for all the wavelengths with the size distribution of urban type<sup>(1)</sup>. In the free troposphere, on the other hand, we assume that the refractive index is  $1.5 - 0.01i$  and the size distribution is of background type<sup>(1)</sup>. The vertical distribution of  $S_1$  is common to all the models. Although we assume a constant  $S_1$  parameter for the entire range of analysis in the reference profile method, we retain its altitude dependence in the calculation of these model profiles. Below, we derive the  $S_1$  parameter in the MBL.

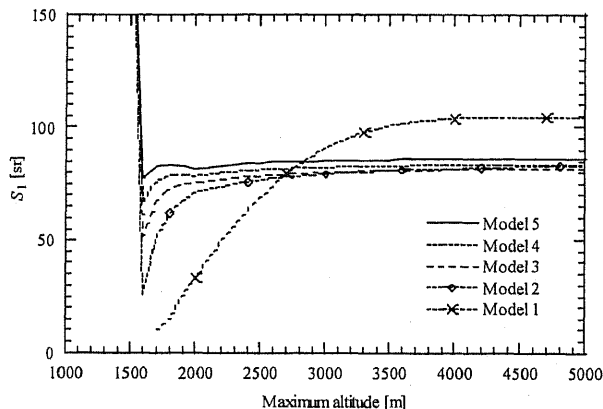


**Figure 1.** Effect of the fitting interval on the retrieval of the  $S_1$  parameter. With a fixed initial altitude of 500 m, the variation of the resulting  $S_1$  parameter is examined for 355 nm by changing the maximum altitude. For models 2-5, reasonable values are obtained for maximum altitudes above 2000 m.

In the reference profile method, the difference between  $\alpha_1^{(\text{Obs})}(S_1, \lambda_j, z)$  and  $\alpha_1^{(\text{Ref})}(\lambda_j, z) = C_j \alpha_1^{(\text{Obs})}(\lambda_{532}, z)$  is considered using  $D_j(S_1)$  in eq. (7). If the interval between the lowest altitude and the maximum altitude is too small, local inhomogeneity in  $\alpha_1^{(\text{Obs})}$  might lead to an error of  $S_1$ . On the contrary, if the maximum altitude is too high, the noise included in  $\alpha_1^{(\text{Obs})}$  (due to the degraded signal-to-noise ratio) may obscure the minimum of  $D_j(S_1)$ . Therefore, here we examine how the fitting of  $S_1$  is influenced by the fitting interval. In the vertical measurement with the ADCL, the lowest altitude (determined by the overlap of the laser beam with the telescope field of view) is approximately 400 m with a telescope field-of-view angle of 3 mrad. Thus, fixing the initial altitude at 500 m, we have studied the variation of the resulting  $S_1$  parameter for 355 nm by changing the maximum altitude. The result is summarized in Fig. 1 for the extinction profiles (models 1-5) mentioned above. As seen from this figure, the behavior for the case of model 2-5 is more or less similar, though it is obviously different for model 1, which has the smallest value of the extinction in the MBL. Since in this latter case the contribution above the MBL becomes more significant, the resultant value of  $S_1$  exhibits noticeable

dependence on the maximum altitude. Although the value saturates above approximately 3500 m, this limiting value has no relation with the MBL value in the original assumption. For models 2-5, on the contrary, the derived values are found to be within  $\pm 15\%$  of the originally assumed value in the MBL ( $S_1 = 74.8$  sr) as long as the maximum altitude is placed above 2000 m.

### 3.1.2. Application of the reference profile method to ADCL data

Here the reference profile method is applied to the actual lidar data measured with the ADCL.

To obtain  $\alpha_1^{(Obs)}(\lambda_j, z)$  using the Fernald method, we assume constant values of extinction coefficients for the altitude range lower than the full overlap altitude of the ADCL. Figure 2 depicts the results for signals observed on October 9, 1998.

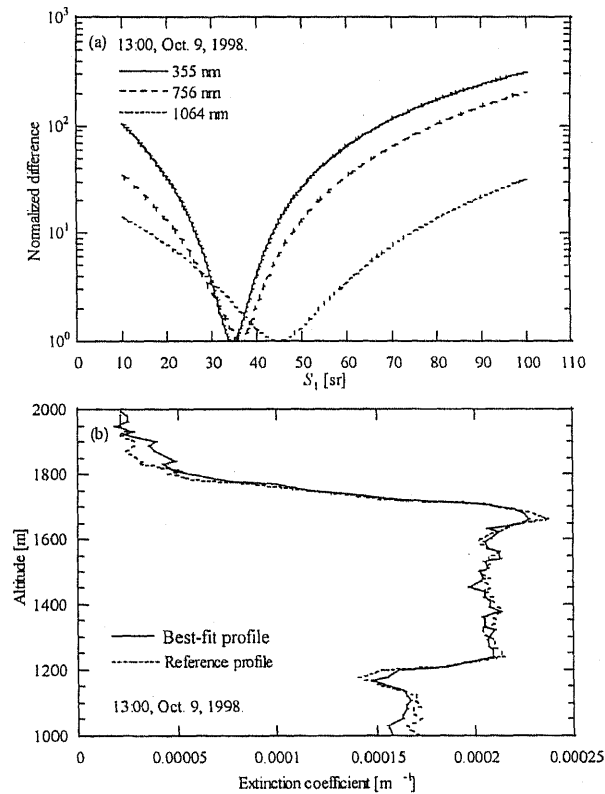


**Figure 2.** Analysis of an ADCL data observed on October 9, 1998. (a) Behavior of the normalized difference  $D_j(S_1)$  as a function of  $S_1$  ( $\lambda_j=355, 756,$  and  $1064$  nm). From the minimum positions of the curves, best-fit values of  $S_1$  are determined. (b) Comparison between the reference profile  $\alpha_1^{(Ref)}(\lambda_{355}, z)$  with the best-fit curve of  $\alpha_1^{(Obs)}(\lambda_{355}, z)$  that minimizes  $D_{355}(S_1)$ .

Figure 2(a) shows the behavior of  $D_j(S_1)$  as a function of  $S_1$  ( $\lambda_j=355, 756,$  and  $1064$  nm). The value of  $D_j(S_1)$  is normalized so that its minimum value becomes unity. The initial and final altitudes of the fitting are set to be 1000 m and 2000 m, respectively. In Fig. 2(b) we plot  $\alpha_1^{(Ref)}(\lambda_{355}, z)$  along with the best-fit profile of  $\alpha_1^{(Obs)}(\lambda_{355}, z)$  that minimizes  $D_{355}(S_1)$ . For 532 nm, the value of the  $S_1$  parameter is 43 sr, as derived from the  $\tau$ -matching method. For the other wavelengths, the best-fit values from this analysis are 34 sr (355 nm), 36 sr (756 nm), and 44 sr (1064 nm). In the case of Fig. 2, the optical thickness at  $\lambda_{532}$  between the altitude of 0 m and 2000 m amounts to 84 % of the total optical thickness. Thus, in accordance with the result in Sec. 3.1.1, the error in the estimation of  $\alpha_1^{(Ref)}$  is small. To check the  $S_1$  values derived from the reference profile method, we derive  $S_1$  by using the separate application of the  $\tau$ -matching method to

each wavelength. The  $S_1$  parameters are obtained to be 31 sr (355 nm), 29 sr (756 nm), and 37 sr (1064 nm), in reasonable agreement with the values from the present analysis.

## 3.2. LUT method

### 3.2.1. Simulation of the LUT method

Since the LUT method basically relies on the wavelength dependence of the signal intensity, it may happen that a noise superposed onto the signal at a particular wavelength at a particular range affects the entire result higher than that altitude. In order to evaluate such a noise effect, here we conduct a sensitivity-analysis simulation assuming a threefold layer. First we prepare the vertical distributions of the extinction coefficients and the  $S_1$  parameters. For the ground layer from 0 to 1000m, we assume the size distribution of the urban aerosol model ( $s = 0$ ) with a relatively large value of the imaginary part of the refractive index of  $m''=0.02$ . For the middle (1000~2000m) and upper (2000~3000m) layers, we assume  $s = 5$  with  $m''=0.01$ , and  $s = 10$  with  $m''=0.0$ , respectively. A noise of 6.5% in magnitude is applied to a data point at 1600 m of the 355 nm  $S_1$  profile, and its effect is examined in the profiles of extinction coefficients and  $S_1$  parameters, as retrieved by the LUT method. This situation is equivalent to the addition of noise in the signal intensity, since with the change in the  $S_1$  the value of the aerosol backscattering is also changed. By assuming that the overlapping function  $G(z)$  takes a value of 1, we calculate the lidar signals for the four wavelengths by use of eq. (1).

The LUT method is applied to the prepared signals. The result shows that for both  $\alpha_1$  and  $S_1$ , the errors at the location of 1600 m are less than 10% in the retrieved profiles. For altitudes higher than the noise location, the errors are found to be less than 1.2%. Therefore, the LUT method is relatively insensitive to the noise if it influences the lidar signal only at a location at a particular wavelength. A similar simulation is carried out for a case in which a 6.5% noise is added at an altitude to two wavelengths. The resulting errors in the  $S_1$  parameters at higher altitudes turn out to be less than 6%.

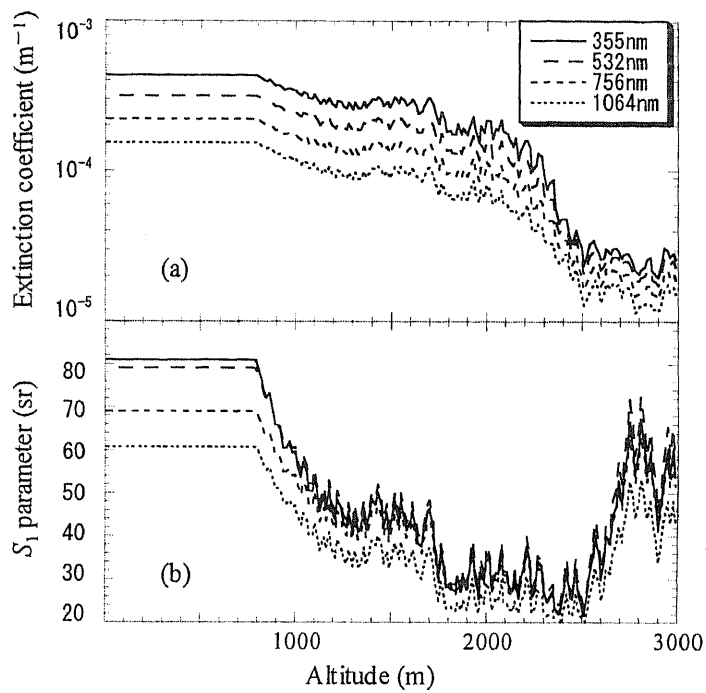
### 3.2.2. Application of the LUT method to ADCL data

The LUT method is applied to the actual lidar data obtained with the ADCL at Chiba University. The data were taken on May 21, 1999 (JST 15:55) with a vertical resolution of 15 m. The results are depicted in Fig. 3.

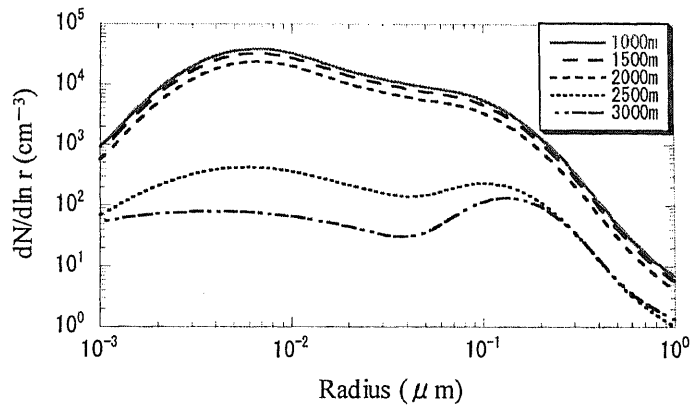
Figure 3(a) shows the vertical profiles of the aerosol extinction for the four wavelengths. It is seen that the mixed layer height is about 2300 m. The altitude dependence of the  $S_1$  parameter is shown in Fig. 3(b). For all the wavelengths, the  $S_1$  values are relatively large near the ground level: the values decrease toward higher altitudes, becoming larger again in the free troposphere. It is also seen that the differences of  $S_1$  among wavelengths tend to decrease as the altitude becomes higher. The  $S_1$  parameter for 532 nm varies in a range of 20~80 sr, with an additional layer-like structure around 1500 m. For this wavelength, previous works have derived  $S_1$  values of 60~70 sr<sup>12)</sup> for continental aerosols using a 180° backscattering nephelometer, 20~70 sr<sup>2)</sup> from the ground observation using a sun photometer, and 75 ± 20 sr<sup>13)</sup> from the vertical distribution of the  $S_1$  parameter determined using a Raman lidar. The present result of 20~80 sr is considered to be reasonable as compared with these previously reported values.

Figure 4 shows the curves of the ASD for five altitudes between 1000 m and 3000 m. Within the mixed layer, it is apparent that the fine (accumulation mode) particles are dominant, and the shape and magnitude of the curves exhibits little changes. In the free troposphere, on the other hand, the relative importance of the coarse mode particles increases, with notable decrease in particle concentrations

In the present method using a LUT, the analysis starts at the near-end boundary. This is in contrast with the case of the Fernald method, in which a far-end boundary value is assumed for the extinction coefficient. Obviously, the present method has the advantage that the signal at the near-end boundary is less likely to be influenced by the detection noise, and as a result, stable convergence of the solution is expected. In Fig. 5, we show the vertical distribution of the aerosol extinction coefficient obtained by applying the Fernald method to the same signals used in Fig. 3. In this case, the inversion is carried out using the  $S_1$  parameters derived from the Mie-scattering calculation with a refractive index of 1.50-0.01i, a value usually assumed for the urban aerosol model.<sup>11)</sup> From Fig. 5, it is seen that the variation of the extinction coefficient is smoother than the case of Fig. 3(a), exhibiting nearly constant values below ~1500 m. Whereas in Fig. 3(a) a layer-like feature is recognizable around 1500 m, no such feature is found in Fig. 5 except one around 3000 m. The extinction coefficients exhibit broad peaks around 2000 m in Fig. 5: the location and height of the peaks, however, are variable in accordance with the choice of the far-end boundary values and  $S_1$  parameters.



**Figure 3.** Results obtained with the LUT method for lidar data observed at Chiba at JST 15:55 on May 21, 1999: (a) aerosol extinction coefficient and (b)  $S_1$  parameter.



**Figure 4.** Altitude dependence of the number size distribution obtained for the data same as in Fig. 3.

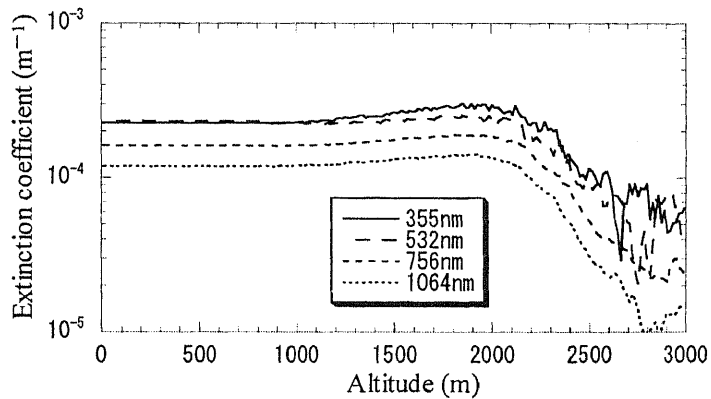


**Figure 5.** Aerosol extinction profile obtained with the Fernald method for the data same as in Fig. 3. The  $S_1$  parameters are assumed to be 49.8, 47.9, 43.3, and 37.9 sr for 355, 532, 756, and 1064 nm, respectively.

#### 4. CONCLUSIONS

We have described the principle, simulation, and practical application of the reference profile method and LUT method to determine the aerosol optical properties from multi-wavelength lidar observations.

In the reference profile method, we choose 532 nm data as a reference, considering the wavelength dependence of the lidar observation range. Auxiliary data obtained by a sun photometer can be applied at this wavelength to calibrate the lidar data. Subsequently, the  $S_1$  parameters for other wavelengths are determined on the basis of reference profiles obtained by scaling the 532 nm profile with appropriate proportional factors. The factors are determined from the sun photometer data for other wavelengths. The application of this algorithm to the actual lidar data obtained with the ADCL gives results comparable to those obtained from the separate determination of the  $S_1$  parameter by using the sun photometer optical thickness at each wavelength. The advantage of the reference profile method consists in the fact that apart from the 532 nm data, it is not required to have "full range" lidar data at other wavelengths. This alleviates the burden on the lidar hardware, allowing the limited range of observation for some wavelengths, due presumably to small laser power or limited detector efficiency. The aerosol properties thus derived from the reference profile method provide convenient bases for the construction of the table in the LUT approach.

In the LUT method, aerosol optical parameters are derived in a height-resolved way through fitting the observed signals to the calculated signals based on the LUT. Better results are expected if the LUT is prepared for parameter ranges as wide as possible. Because of the limit in the computation time, however, our calculation is performed for 11 types of ASD (varying between urban and maritime model) and 3000 values of the imaginary part of the refractive index ( $m''=0.0\sim 0.03$ ). Thus, good knowledge about the plausible ranges in which aerosol properties may change is prerequisite for the effective implementation of the method.

#### REFERENCES

1. F. G. Fernald, "Analysis of atmospheric lidar observations: some comments," *Appl. Opt.*, **23**, pp. 652–653, 1984.
2. T. Takamura, Y. Sasano, and T. Hayasaka, "Tropospheric aerosol optical properties derived from lidar, sun photometer, and optical particle counter measurements," *Appl. Opt.*, **33**, pp. 7132–7140, 1994.
3. H. C. van de Hulst, *Light scattering by Small Particles*, pp. 114–171, Dover, New York, 1957.
4. Y. Sasano and E.V. Browell, "Light scattering characteristics of various aerosol types derived from multiwavelength lidar observations," *Appl. Opt.*, **28**, pp. 1670–1679, 1989.
5. P. Qing, H. Nakane, Y. Sasano, and S. Kitamura, "Numerical simulation of the retrieval of aerosol size distribution from multiwavelength laser radar measurements," *Appl. Opt.*, **28**, pp. 5259–5265, 1989.
6. K. Rajeev and K. Parameswaran, "Iterative method for the inversion of multiwavelength lidar signals to determine aerosol size distribution," *Appl. Opt.*, **37**, pp. 4690–4700, 1998.
7. N. Takeuchi, H. Kuze, Y. Sakurada, T. Takamura, S. Murata, K. Abe and S. Moody: *Proc. 18th Int. Conf. Laser Radar, Berlin, 1996* (Springer-Verlag, Berlin, 1997) p. 71.
8. H. Kuze, M. Qiang, Y. Sakurada, T. Takamura, and N. Takeuchi: *Proc. 18th Int. Conf. Laser Radar, Berlin, 1996* (Springer-Verlag, Berlin, 1997) p. 75.
9. H. Kinjo, H. Kuze, T. Takamura, M. Yabuki, and N. Takeuchi: "Determination of aerosol extinction-to-backscattering Ratio from Multiwavelength lidar observation," *J. J. Appl. Phys.*, **40**, in press.
10. M. Yabuki, H. Kuze, H. Kinjo, and N. Takeuchi: *J. J. Appl. Phys.*, to be submitted.
11. R. Jaeniche, *Tropospheric Aerosols*, in Peter V. Hobbs ed., *Aerosol-Cloud-Climate Interactions*, pp. 1–31, Academic, 1983.
12. S. J. Doherty, T. L. Anderson, and R. J. Charlson, "Measurement of the lidar ratio for atmospheric aerosols with 180° backscatter nephelometer," *Appl. Opt.*, **38**, pp. 1823–1832, 1999.
13. D. Muller, U. Wandinger, D. Aithausen, I. Mattis, and A. Ansmann, "Retrieval of physical particles from lidar observations of extinction and backscatter at multiple wavelengths," *Appl. Opt.*, **37**, pp. 2260–2262, 1998.